A cellular basis of human intelligence

Natalia A. Goriounova[1,*], Djai B. Heyer[1,**], René Wilbers[1,**], Matthijs B. Verhoog[1], Michele Giugliano[2,3,4], Christophe Verbist [2], Joshua Obermayer[1], Amber Kerkhofs[1], Harriët Smeding[5], Maaike Verberne[5], Sander Idema[6], Johannes C. Baayen[6], Anton W. Pieneman[1], Christiaan P.J. de Kock[1], Martin Klein[7], Huibert D. Mansvelder[1]

[1]Department of Integrative Neurophysiology, Amsterdam Neuroscience, Center for Neurogenomics and Cognitive Research (CNCR), Vrije Universiteit Amsterdam, De Boelelaan 1085, Amsterdam 1081 HV, the Netherlands.

[2] Molecular, Cellular, and Network Excitability Lab, Dept. of Biomedical Sciences, University of Antwerp, Antwerp, Belgium

[3] Department of Computer Science, University of Sheffield, S1 4DP Sheffield, UK

[4] Lab of Neural Microcircuitry, Brain Mind Institute, EPFL, CH-1015 Lausanne, Switzerland

[5]Department of Psychology, Stichting Epilepsie Instellingen Nederland (SEIN), Achterweg 5, 2103 SW Heemstede & Dr. Denekampweg 20, 8025 BV Zwolle, the Netherlands.

[6]Department of Neurosurgery, Amsterdam Neuroscience, VU University Medical Center, De Boelelaan 1117, Amsterdam 1081 HV, the Netherlands.

[7]Department of Medical Psychology, Amsterdam Neuroscience, VU University Medical Center, De Boelelaan 1118, Amsterdam 1081 HZ, the Netherlands.

[*]Correspondence to: n.a.goriounova@vu.nl

[**]Equal contribution.

Abstract

It is generally assumed that human intelligence relies on efficient processing by neurons in our brain. Although gray matter thickness and activity of temporal and frontal cortical areas correlate with IQ scores, no direct evidence exists that links structural and physiological properties of neurons to human intelligence. Here, we find that high IQ scores and large temporal cortical thickness associate with larger, more complex dendrites of human pyramidal neurons. We show *in silico* that larger dendritic trees enable pyramidal neurons to track activity of synaptic inputs with higher temporal precision, due to fast action potential kinetics. Indeed, we find that human pyramidal neurons of individuals with higher IQ scores sustain fast action potential kinetics during repeated firing. These findings provide the first evidence that human intelligence is associated with neuronal complexity, action potential kinetics and efficient information transfer from inputs to output within cortical neurons.

Introduction

A fundamental questions in neuroscience is what properties of neurons lie at the heart of human intelligence and underlie individual differences in mental ability. Thus far, experimental research on the neurobiological basis of intelligence has ignored the neuronal level and has not directly tested what role human neurons play in cognitive ability, mainly due to the inaccessibility of human neurons. Instead, research has either been focused on finding genetic loci that can explain part of the variance in intelligence (Spearman's *g*) in large cohorts (Lam et al., 2017; Sniekers et al., 2017; Trampush et al., 2017) or on identifying brain regions in whole brain imaging studies of which structure or function correlate with IQ scores (Choi et al., 2008; Deary et al., 2010; Karama et al., 2009a; McDaniel, 2005; Narr et al., 2007). Some studies have highlighted that variability in brain volume and intelligence may share a common genetic origin (Hulshoff Pol et al., 2006; Posthuma et al., 2002; Sniekers et al., 2017), and individual genes that were identified as associated with IQ scores might aid intelligence by facilitating neuron growth (Sniekers et al., 2017) and directly influencing neuronal firing (Lam et al., 2017).

Intelligence is a distributed function that depends on activity of multiple brain regions (Deary et al., 2010). Structural and functional magnetic resonance imaging studies in hundreds of healthy subjects revealed that cortical volume and function of specific areas correlate with *g* (Choi et al., 2008; Karama et al., 2009a; Narr et al., 2007). In particular, areas located in the frontal and temporal cortex show a strong correlation of grey matter thickness and functional activation with IQ scores: individuals with high IQ show larger grey matter volume of, for instance, Brodmann areas 21 and 38 (Choi et al., 2008; Deary et al., 2010; Karama et al., 2009b; McDaniel, 2005; Narr et al., 2007). Cortical grey matter consists for a substantial part of dendrites (Chklovskii et al., 2002; Ikari and Hayashi, 1981), which receive and integrate synaptic information and strongly affect functional properties of neurons (Bekkers and Häusser, 2007; Eyal et al., 2014; Vetter et al., 2001). Especially high-order association areas in temporal and

frontal lobes in humans harbour pyramidal neurons of extraordinary dendritic size and complexity (Elston, 2003; Mohan et al., 2015) that may constitute variation in cortical thickness, neuronal function, and ultimately IQ. These neurons and their connections form the principal building blocks for coding, processing, and storage of information in the brain and ultimately give rise to cognition (Salinas and Sejnowski, 2001). Given their vast number in the human neocortex, even the slightest changes in the efficiency of information transfer by neurons may translate into large differences in mental ability. However, whether and how the activity and structure of single human neurons support human intelligence has not been tested.

To investigate whether structural and functional properties of neurons of the human temporal cortex associate with general intelligence, we collected a unique multimodal data set from human subjects containing single cell physiology, neuronal morphology, pre-surgical MRI scans and IQ test scores (Fig 1). We recorded action potentials (APs) from human pyramidal neurons in superficial layers of temporal cortical tissue resected during neurosurgery (Brodmann areas 38 and 21) and digitally reconstructed their complete dendritic structures. We tested the hypothesis that variation in neuronal morphology and function can explain variation in IQ scores and used computional modelling to understand underlying principles of efficient information transfer in cortical neurons and networks.

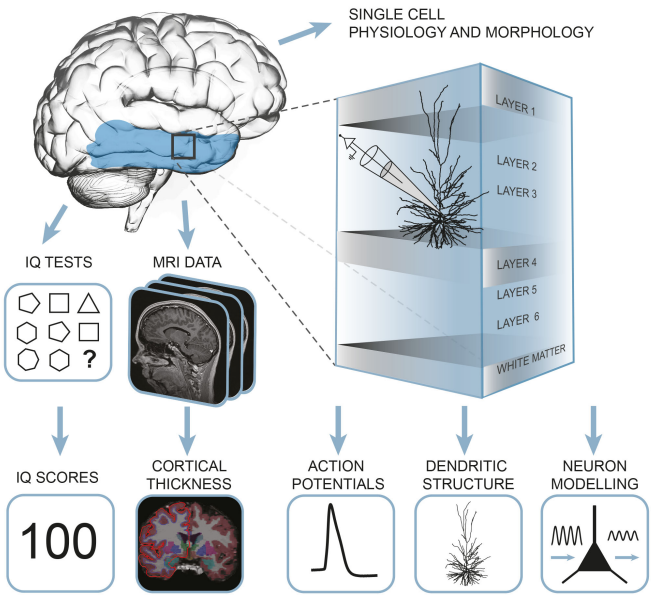

Figure 1. Summary of the approach: multidimensional data set from human subjects contained single cell physiology, neuronal morphology, MRI and IQ test scores (WAIS FSIQ). The area of the brain highlighted in blue indicates the location of cortical thickness measurements, black square indicates the tipical origin or resected cortical tissue.

Results

IQ scores positively correlate with cortical thickness of the temporal lobe

Cortical thickness of the temporal lobe has been associated with IQ scores in hundreds of subjects (Choi et al., 2008; Deary et al., 2010; Hulshoff Pol et al., 2006; Karama et al., 2009a; Narr et al., 2007) and we first asked whether this applies to the subjects in our study as well. From T1-weighted MRI scans obtained prior to surgery, we determined temporal cortical thickness in 35 subjects using voxel-based morphometry. We selected temporal cortical areas corresponding to surgical resections (Fig 2A) and collapsed the measurements for temporal lobes to one mean value for cortical thickness for each subject. In line with previous studies (Choi et al., 2008; Deary et al., 2010; Hulshoff Pol et al., 2006; Karama et al., 2009b; Narr et al., 2007), mean cortical thickness in temporal lobes positively correlated with IQ scores of the subjects (Fig 2B).

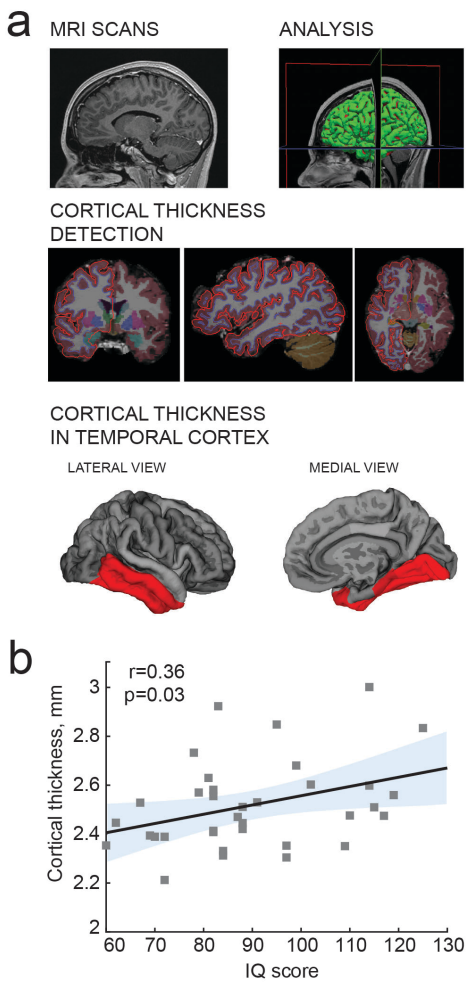

Figure 2. IQ scores positively correlate with cortical thickness of the temporal lobe. (**a**) MRI analysis pipeline: 1) Presurgical MRI T1-weighted scans; 2) Morphometric analysis; 3) Detection of cortical thickness from pial and white-grey matter boundaries; 4) selection of temporal cortical area for correlations with IQ in B (highlighted in red). (**b**) Average cortical thickness in temporal lobe (from area highlighted in red in A4) positively correlates with IQ scores form the same subjects (n

subjects=35). Here and further, Pearson correlation coefficients and p-values are reported in graph insets, blue highlighter area indicates 95% confidence bounds of the fit.

IQ scores positively correlate with dendritic structure of temporal cortical pyramidal cells

Cortical association areas in temporal lobes play a key role in high-level integrative neuronal processes and superficial layers harbour neurons of increased neuronal complexity (DeFelipe et al., 2002; Elston, 2003; Scholtens et al., 2014; van den Heuvel et al., 2015). In rodents, the neuropil of cortical association areas consists for over 30% of dendritic structures (Ikari and Hayashi, 1981). To test whether human temporal cortical thickness is associated with dendrite size, we used 68 full reconstructions of biocytin-labelled temporal cortical pyramidal neurons from human layer 2, 3 and 4 previously reported (Mohan et al., 2015). Surgically obtained cortical tissue was non-pathological, and was resected to gain access to deeper structures containing disease focus (Mohan et al., 2015; Testa-Silva et al., 2010; 2014; Verhoog et al., 2013; 2016) (typically medial temporal sclerosis or hippocampal tumour; Table S1). In line with the non-pathological status of tissue, we observed no correlations of cellular parameters or IQ scores with the subject's disease history and age (Fig S1&S2). We calculated total dendritic length (TDL) for each neuron and mean TDL from multiple cells for each subject and correlated these mean TDL values (n=23 subjects) to mean temporal cortical thickness from the same subject. We found that dendritic length positively correlated with mean temporal lobe cortical thickness, indicating that dendritic structure of individual neurons contributes to the overall cytoarchitecture of temporal cortex (Fig 3A).

TDL is in part determined by the soma location within cortical layers: cell bodies of pyramidal neurons with larger dendrites typically lie deeper, at larger distance from pia (Mohan et al., 2015). Thus, differences in soma locations of targeted neurons from subject to subject may result in biased sampling. To exclude a systematic bias in sampling, we determined the

cortical depth of each neuron recorded from relative to the subject's temporal cortical thickness in the same hemisphere. There was no correlation between IQ score and relative cortical depth of pyramidal neurons used in this study, indicating that TDL was determined from neurons at similar depths across subjects (Fig 3B). Finally, we tested whether mean TDL and complexity of pyramidal neurons relates to subjects' IQ scores. We found a strong positive correlation between individual's pyramidal neuron TDL and IQ scores (Fig 3C) as well as between number of dendritic branch points and IQ scores (Fig 3D), thus revealing a significant association between human intelligence and dendritic length and complexity.

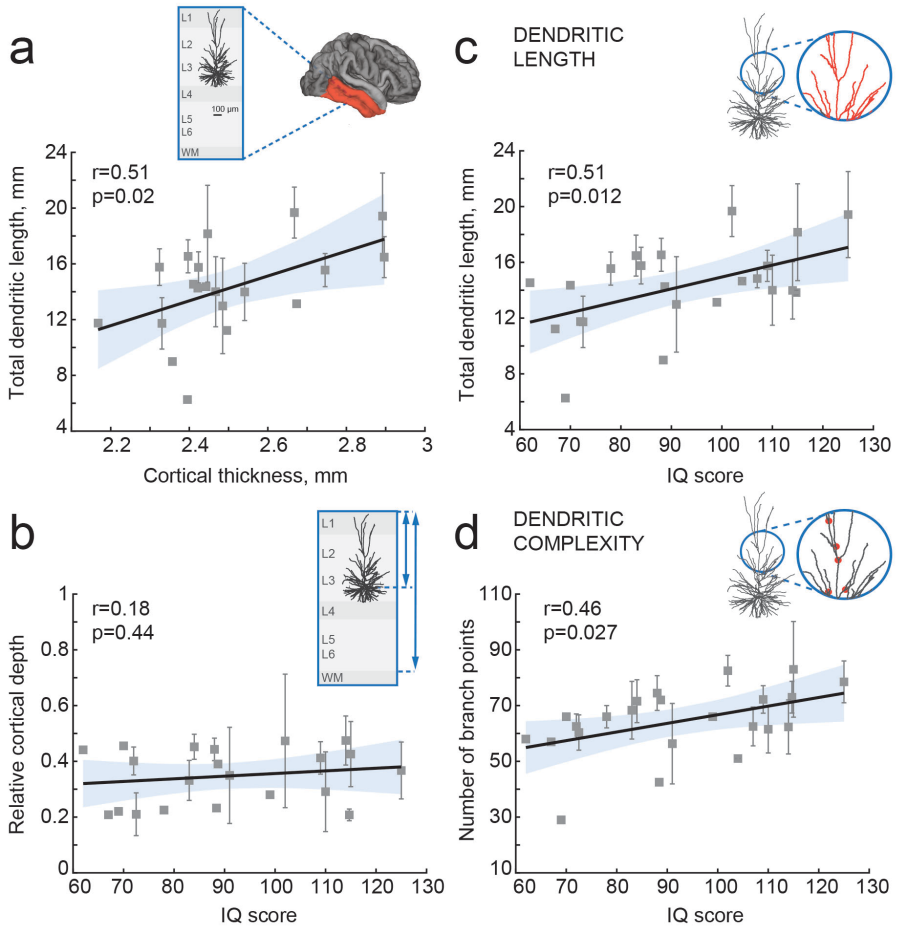

Figure 3. IQ scores positively correlate with dendritic structure of temporal cortical pyramidal cells. (**a**) Average total dendritic length in pyramidal cells in superficial layers of temporal cortex positively correlates with cortical thickness in temporal lobe from the same hemisphere (area highlighted in A, n subjects=20; n

cell=58). Inset shows a scheme of cortical tissue with a digitally reconstructed neuron and the brain area for cortical thickness estimation (red) (**b**) Cortical depth of pyramidal neurons, relative to cortical thickness in temporal cortex from the same hemisphere, does not correlate with IQ score (n subjects=21). Inset represent the coritical tissue, blue lines indicate the depth of neuron and cotical thickness (**c**) Pyrmidal cell TDL and (**d**) number of dendritic brainch points positively correlate with IQ scores from the same individuals (n subjects=23, n cells=68).

Larger dendrites lead to faster AP onset and improved encoding properties

Dendrites not only receive most synapses in neurons, but dendritic morphology and conductances act in concert to regulate neuronal excitability (Bekkers and Häusser, 2007; Eyal et al., 2014; Vetter et al., 2001). Increase in the size of dendritic compartment *in silico* was shown to accelerate APs and improve encoding capability of simplified model neurons (Eyal et al., 2014). Further, human neocortical pyramidal neurons, which are three times larger than rodent pyramidal neurons (Mohan et al., 2015), have faster AP onsets compared to rodent neurons and are able to track fast-varying inputs with high temporal precision (Testa-Silva et al., 2014). We asked whether the observed differences in TDL between human pyramidal neurons affected their encoding properties. To this end, we incorporated the 3-dimensional dendritic reconstructions of the human pyramidal neurons into *in silico* models and equipped them with excitable properties (see the Supplemental Methods). Larger TDL led to faster AP onsets in the model neurons (Fig. 4 a,b). Faster APs would imply that neurons can respond faster to synaptic inputs, thereby can translate higher frequencies of synaptic membrane potential fluctuations into action potential timing and ultimately encode more information. We tested this by simulating current inputs of increasing frequencies into modelled neurons and studied how firing of the modelled neurons followed input changes. Human neurons with larger TDL could reliably transfer high frequency ranges, with cut-off frequencies up to 400-500 Hz, while smaller neurons had their cut-off frequencies already at 200 Hz (Fig 4c, d). Furthermore, there was a

significant positive correlation between the dendritic length and the cut-off frequency (Fig. 4d). Finally, given the same input - composed of the sum of three sinusoids of increasing frequencies - larger neurons were able to better encode rapidly changing temporal information in firing output, compared to smaller cells (Fig. 4e). Thus, we find that *in silico*, structural differences in dendritic length of reconstructed human neurons lead to faster APs and thereby to higher frequency bandwidths of encoding synaptic inputs in AP output.

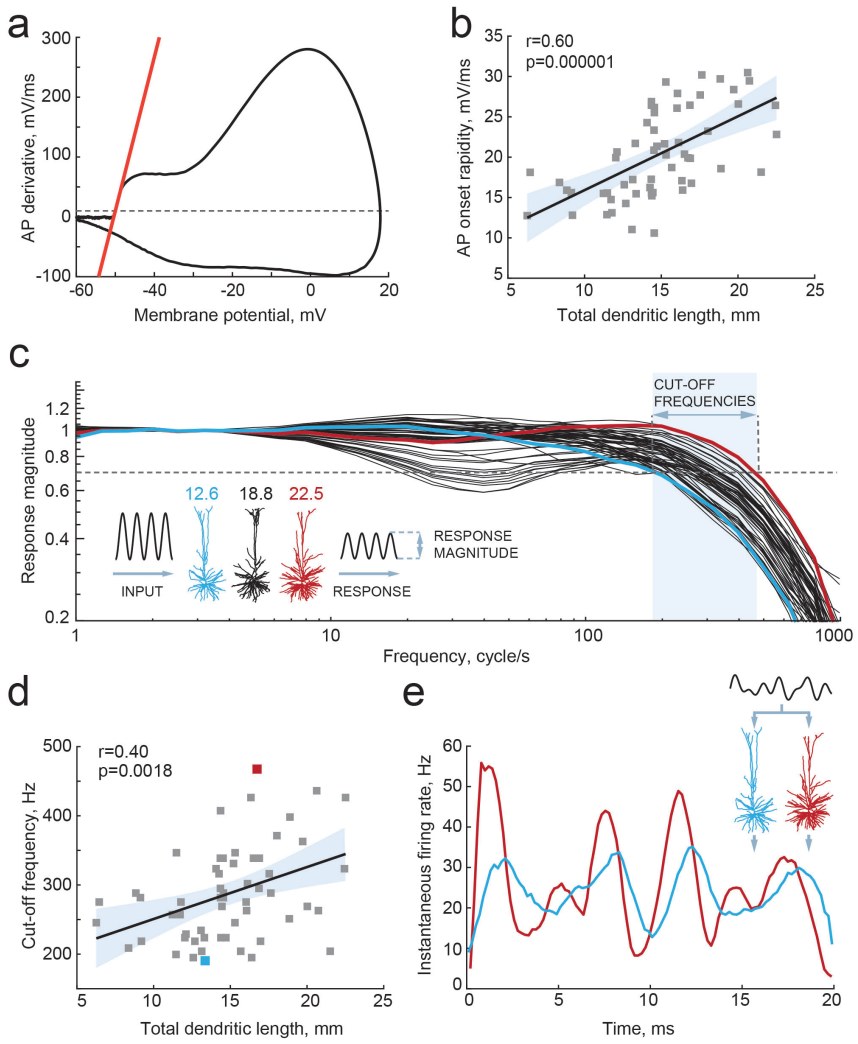

Figure 4. Larger dendrites lead to faster AP onset and improved encoding properties. (**a,b**) Higher TDL results in faster onsets of model-generated APs: **(a)** example phase plot of an AP is shown with a red line

representing onset rapidity - slope of AP derivative at 10 mV/ms (grey dashed line)**; (b)** onset rapidity values of simulated APs positively correlate with TDL. **(c)** Model neurons received simulated sinusoidal current-clamp inputs and generated spiking responses of different magnitudes and frequencies. Red and blue traces are response magnitudes of example neurons with low (blue) and large (red) TDLs; inset shows their morphological reconstructions and TDLs. Cut-off frequencies are defined within the frequency range (highlighted in blue) at which model neuron can still track the inputs reliably (produce response of 0.7 response magnitude, dashed line). (**d**) Cut-off frequencies positively correlate with TDL (example neurons from panel (**c**) are marked by the same colors). (**e**) Responses to the same input in two example neurons from panels **(b)** and **(c):** instantaneous firing frequency of the model neuron with large TDL (red) follows the input with higher temporal precision than model neuron with smaller TDL (blue).

Higher IQ scores associate with faster AP kinetics and lower firing threshold

We next asked whether human cortical pyramidal neurons from individuals with higher IQ scores show faster AP kinetics during repeated AP firing. To test this, we made whole-cell recordings from pyramidal cells in acute slices of temporal cortex (26 subjects, 101 cells, 10,538 APs; Fig 5A) and recorded APs at different firing frequencies in response to depolarising current steps. We analysed the kinetics of all APs and grouped them based on instantaneous firing frequency of each AP to investigate the changes in waveforms of APs during increasing neuronal activity. Next, we split all AP data into two groups based on IQ score – above and below 100 – and observed more pronounced changes in AP kinetics in individuals with lower IQ score: their APs showed a substantial slowing of kinetics starting at instantaneous firing frequencies as low as 10 Hz (Fig 5B). To statistically test the differences between the IQ groups in AP kinetics, we extracted key AP parameters – peak voltage, amplitude, threshold, afterhyperpolarization, maximum rise speed, maximum fall speed and half-width (Tabel S2) – and normalized these parameters for each AP to the first APs in the traces. Since the slowing of APs was already prominent at low firing frequencies, we grouped all APs for instantaneous

frequencies of 11-50 Hz, and ran MANOVA analysis with the seven AP parameters. MANOVA confirmed significant difference in AP properties between higher and lower IQ groups ($F(7,18) = 3.037$, $p = 0.027$), with univariate post hoc tests narrowing the significant results to AP threshold, rise speed, fall speed and half-width (Fig 5C). These AP parameters were more affected by higher frequency firing in subjects with lower IQ than in subjects with higher IQ. Specifically, AP threshold increased significantly more compared to subjects with higher IQ, indicating that it is progressively more difficult to evoke APs during repeated neuronal activity in these neurons. In addition, APs from subjects with lower IQ slowed significantly more: their rise and fall speeds decreased while AP duration (half-width) increased (Fig 5C).

We further investigated whether these differences at the group level reflected correlations between individual IQ scores and AP kinetics. We correlated IQ scores to mean relative AP thresholds, rise and fall speeds and half-widths at 11-50 Hz from all neurons of the same subject. All four parameters showed strong correlations with IQ (Fig 5D). During repeated firing, AP threshold and half-width relative to the first AP negatively correlated with IQ scores, while AP rise and fall speed showed strong positive correlations (Fig 5D). These findings indicate that higher IQ scores link to low AP firing threshold and fast kinetics during repeated AP firing, while lower IQ scores associate with increased AP fatigue during elevated neuronal activity. Our results indicate that neurons from individuals with higher IQ scores are better equipped to process synaptic signals at high rates and at faster time scales, which is necessary to encode large amounts of information accurately and efficiently.

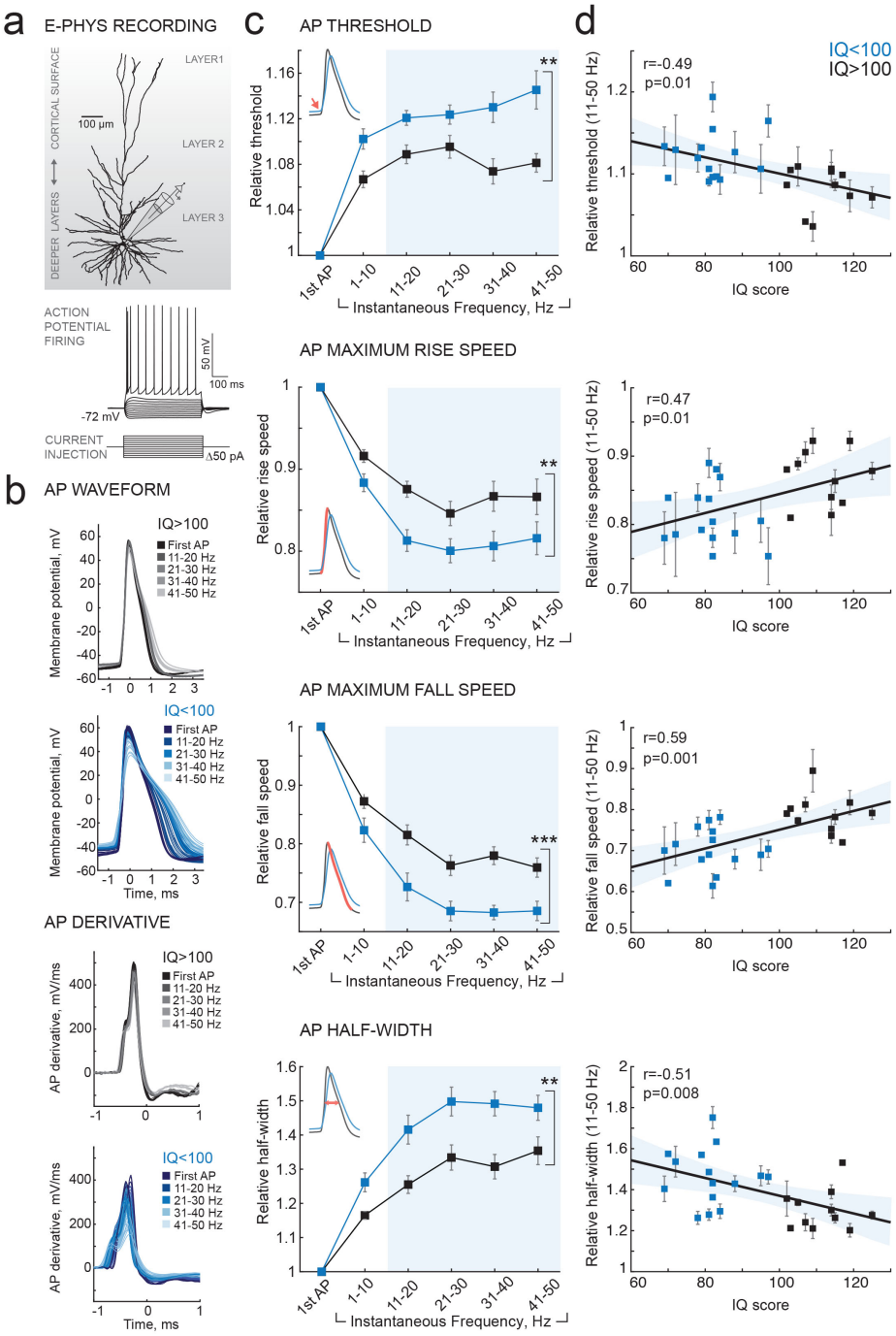

Figure 5. Higher IQ scores associate with faster AP kinetics and lower firing threshold**.** (**a**) Scheme of a whole-cell recording showing biocytin reconstruction of a layer 2/3 pyramidal neuron from human temporal cortex. Right: typical voltage responses to depolarizing somatic current injections. (**b**) AP waveforms and derivatives at increasing instantaneous firing frequencies (colour code in insets) recorded from a subject with IQ<100 (blue) and a subject with IQ>100 (black). Traces are aligned to the timing of AP peak. (**c**)

Average relative AP threshold, rise and fall speeds and half-width in neurons from subjects with lower IQ (black, n subjects=11, n cells=49) and subjects with higher IQ (blue, n subjects=15, n cells=52) displayed against instantaneous firing frequency. In subjects with higher IQ AP threshold and AP kinetics were less affected by higher frequencies: there was less increase in AP threshold, less slowing of rise and fall speeds and less elongation of AP half-width. (MANOVA univariate comparisons on mean values for 11-50Hz, highlighted in blue; Bonferroni corrected $p<0.007$; threshold $F(1,24)=13.325$, $p=0.001$; rise $F(1,24)=10.086$, $p=0.004$; fall $F(1,24)= 21.989$, $p<0.001$; half-width $F(1,24)=13.78$, $p=0.001$). Insets represent the measured parameters. **p<0.01, ***p<0.001. (**d**) Average relative AP threshold, half-width, rise and fall speeds at 11-50 Hz (data highlighted in blue in C) correlate with IQ scores (n subjects=26, n cells=101). Data are mean ± SEM.

Discussion

Our findings provide a first insight into the cellular nature of human intelligence and explain individual variation in IQ scores based on neuronal properties: faster AP kinetics during neuronal activity, lower firing thresholds and more complex, extended dendrites associate with higher intelligence. AP kinetics have profound consequences for information processing. In vivo, neurons are constantly bombarded by high frequency synaptic inputs and the capacity of neurons to keep track and phase lock to these inputs determines how much of this synaptic information can be transferred (Testa-Silva et al., 2014). The brain operates at a millisecond time-scale and even sub-millisecond details of spike trains contain behaviourally relevant information that can steer behavioral responses (Nemenman et al., 2008). Indeed, one of the most robust and replicable findings in behavioural psychology is the association of intelligence scores with measures of cognitive information-processing speed (Barrett et al., 1986). Specifically, reaction times (RT) in simple RT tasks provide a better prediction of IQ than other speed-of-processing tests, with a regression coefficient of 0.447 (Vernon, 1983). In addition, high postitive correlations between RT and other speed-of-processing tests suggest the excistence of a common mental speed factor (Vernon, 1983). Our results provide a biological cellular explanation for such mental speed factors: in conditions of increased mental activity, neurons of individuals with higher IQ are able to sustain fast action potentials and can transfer larger cellular information content from synaptic input to AP output.

Pyramidal cells are integrators and accumulators of synaptic information. Larger dendrites can physically contain more synaptic contacts and integrate more information. Indeed, human pyramidal neuron dendrites receive twice as many synapses as in rodents (DeFelipe et al., 2002) and cortico-cortical whole-brain connectivity positively correlates with the size of dendrites in these cells (Scholtens et al., 2014; van den Heuvel et al., 2015). A gradient in complexity of pyramidal cells in cortical superficial layers accompanies the increasing

integration capacity of cortical areas, indicating that larger dendrites are required for higher-order cortical processing (Elston, 2003; van den Heuvel et al., 2015). Our results align well with these findings, suggesting that the neuronal complexity gradient also exists from individual to individual and could explain differences in mental ability.

Larger dendrites have an impact on excitability of cells (Bekkers and Häusser, 2007; Vetter et al., 2001) and determine the shape and rapidity of APs (Eyal et al., 2014). Increasing the size of dendritic compartments *in silico* lead to acceleration of AP onset and increased encoding capability of neurons (Eyal et al., 2014). In the present study, by modeling detailed morphological reconstructions of neurons from human subjects, showed that individuals with larger dendrites are better equipped to transfer synaptic information at higher frequencies. Remarkably, dendritic morphology, AP kinetics and firing threshold are also parameters that we have previously identified as showing pronounced differences between humans and other species (Mohan et al., 2015; Testa-Silva et al., 2014). Human pyramidal cells in layers 2/3 have 3-fold larger and more complex dendrites than in macaque or mouse (Mohan et al., 2015). Moreover, human APs have lower firing threshold and faster AP onset kinetics both in single APs and during repeated firing (Testa-Silva et al., 2014). These differences across species may suggest evolutionary pressure on both dendritic structure and AP waveform and emphasize adaptations of human pyramidal cells in association areas for cognitive functions.

Recent genome-wide association studies (GWAS) have pinpointed genes associated with intelligence that provide potential biological links to neuron development and neuronal activity (Lam et al., 2017; Sniekers et al., 2017; Trampush et al., 2017). For example, GWAS-based pathway analysis identified two gene targets of drugs that affect voltage-gated ion channels associated with general cognitive ability: a T-type calcium channel and a potassium channel (Lam et al., 2017). Both ion channel types play a critical role in determining AP shape and kinetics. T-type calcium channels are involved in action potential initiation and switching

between distinct modes of firing (Cain and Snutch, 2010), while potassium channels are responsible for rapid repolarization during AP generation (Hodgkin and Huxley, 1952). The strongest emerging association of genes with intelligence is an intronic region of the *FOXO3* gene and its promoter (Sniekers et al., 2017), involved in insulin growth factor 1 (IGF-1) signalling pathway (Costales and Kolevzon, 2016). Low IGF-1 levels have been associated with poor cognitive function during aging (Tumati et al., 2016) and a less integrated functional network of connected brain areas (Sorrentino et al., 2017). Notably, one of the effects of IGF-I on cortical pyramidal cells is the increased branching and total size of dendrites (Niblock et al., 2000). Thus, individual differences in gene polymorphisms involved in neuronal development and associated with intelligence could result in larger and more complex dendrites contributing to faster firing of cortical neurons. Ultimately, these genes provide a genetic disposition for a higher encoding bandwidth and information transfer of pyramidal neurons in association areas such as the temporal cortex, gaining a speed advantage in mental processing leading to faster reaction times and higher IQ scores.

Methods

Human subjects and brain tissue

All procedures were performed with the approval of the Medical Ethical Committee of the VU University Medical Centre, and in accordance with Dutch licence procedures and the Declaration of Helsinki. Written informed consent was provided by all subjects for data and tissue use for scientific research. All data were anonymized.

Human cortical brain tissue was removed as a part of surgical treatment of the subject in order to get access to a disease focus in deeper brain structures (hippocampus or amygdala) and typically originated from gyrus temporalis medium (Brodmann areas 21 or 38, occasionally gyrus temporalis inferior or gyrus temporalis superior). Speech areas were avoided during resection surgery through functional mapping. We obtained neocortical tissue from 37 patients (19 females, 18 males; age range 18–66 years, Supplementary table 1) treated for mesial temporal sclerosis, removal of a hippocampal tumour, low grade hippocampal lesion, cavernoma or other unspecified temporal lobe pathology. From 35 of these patients we also obtained pre-surgical MRI scans, from 26 patients we recorded Action Potentials from 101 cells (10,538 APs) and from 23 patients we had fully reconstructed dendritic morphologies from 68 cells. In all patients, the resected neocortical tissue was not part of epileptic focus or tumour and displayed no structural/functional abnormalities in preoperative MRI investigation, electrophysiological whole-cell recordings or microscopic investigation of stained tissue.

IQ scores

Total IQ scores were obtained from the Dutch version of Wechsler Adult Intelligence Scale-III (WAIS-III) and in some cases WAIS-IV. The tests were performed as a part of neuropsychological examination shortly before surgery, typically within one week.

MRI data and cortical thickness estimation

T1-weighted brain images (1 mm thickness) were acquired with a 3T MR system (Signa HDXt, General Electric, Milwaukee, Wisconsin) as a part of pre-surgical assessment (number of slices=170-180). Cortical reconstruction and volumetric segmentation was performed with the Freesurfer image analysis suite (http://freesurfer.net)(Fischl and Dale, 2000). The processing included motion correction, transformation to the Talairach frame. Calculation of the cortical thickness was done as the closest distance from the grey/white boundary to the grey/CSF boundary at each vertex and was based both on intensity and continuity information from the entire three dimensional MR volume (Fischl and Dale, 2000). Neuroanatomical labels were automatically assigned to brain areas based on Destrieux cortical atlas parcellation as described in (Fischl, 2004). For averaging, the regions in temporal lobes were selected based on Destrieux cortical atlas parcellation in each subject.

Slice preparation

Upon surgical resection, the cortical tissue block was immediately transferred to ice-cold artificial cerebral spinal fluid (aCSF) containing in (mM): 110 choline chloride, 26 $NaHCO_3$, 10 D-glucose, 11.6 sodium ascorbate, 7 $MgCl_2$, 3.1 sodium pyruvate, 2.5 KCl, 1.25 NaH_2PO_4, and 0.5 $CaCl_2$ (300 mOsm) and transported to the neurophysiology laboratory (within 500 m from the operating room). The transition time between resection of the tissue and the start of preparing slices was less than 15 minutes. After removing the pia and identifying the pia-white matter axis, neocortical slices (350 mm thickness) were prepared in ice-cold slicing solution (same composition as described above). Slices were then transferred to holding chambers in which they were stored for 30 minutes at 34 C^o and for 30 minutes at room temperature before recording in aCSF, which contained (in mM): 126 NaCl; 3 KCl; 1 NaH_2PO_4; 1 $MgSO_4$; 2 $CaCl_2$; 26 $NaHCO_3$; 10 glucose (300 mOsm), bubbled with carbogen gas (95% O_2/5% CO_2), as described previously (Mohan et al., 2015; Testa-Silva et al., 2010; 2014; Verhoog et al., 2013; 2016).

Electrophysiological recordings

Cortical slices were visualized using infrared differential interference contrast (IR-DIC) microscopy. After the whole cell configuration was established, membrane potential responses to steps of current injection (step size 30-50 pA) were recorded. None of the neurons showed spontaneous epileptiform spiking activity. Recordings were made using Multiclamp 700A/B amplifiers (Axon Instruments) sampling at frequencies of 10 to 50 kHz, and lowpass filtered at 10 to 30 kHz. Recordings were digitized by pClamp software (Axon) and later analyzed off-line using custom-written Matlab scripts (MathWorks). Patch pipettes (3–5 MOhms) were pulled from standard-wall borosilicate capillaries and filled with intracellular solution containing (in mM): 110 K-gluconate; 10 KCl; 10 HEPES; 10 K-phosphocreatine; 4 ATP-Mg; 0.4 GTP, pH adjusted to 7.2–7.3 with KOH; 285–290 mOsm, 0.5 mg/ml biocytin. All experiments were performed at 32C^{o}–35C^{o}. Only cells with bridge balance of <15 MOhm were used for further analysis.

Morphological analysis

During electrophysiological recordings, cells were loaded with biocytin through the recording pipette. After the recordings the slices were fixed in 4% paraformaldehyde and the recorded cells were revealed with the chromogen 3,3-diaminobenzidine (DAB) tetrahydrochloride using the avidin–biotin–peroxidase method (Horikawa and Armstrong, 1988). Slices were mounted on slides and embedded in mowiol (Clariant GmbH, Frankfurt am Main, Germany). Neurons without apparent slicing artifacts and uniform biocytin signal were digitally reconstructed using Neurolucida software (Microbrightfield, Williston, VT, USA), using a ×100 oil objective. After reconstruction, morphologies were checked for accurate reconstruction in x/y/z planes, dendritic diameter, and continuity of dendrites. Finally, reconstructions were checked using an overlay in Adobe Illustrator between the Neurolucida reconstruction and Z-stack projection image from Surveyor Software (Chromaphor, Oberhausen, Germany).

Layer 2/3 pyramidal neurons were identified based on morphological and electrophysiological criteria at cortical depth within 250-1200 μm from cortical surface, that we previously found to correspond to cortical layers 2/3 in humans (Mohan et al., 2015). For each neuron, we extracted total dendritic length (TDL) and number of branch points and computed average TDL and average number of branch points for each subject by pulling data from all cells from one subject (1 to 8 cells per subject).

Neuronal modelling

We constructed multicompartmental spiking neuronal models of human L2/3 pyramidal neurons for each the digitally reconstructed 3-dimensional morphologies considered in this study. Models were simulated using NEURON (Carnevale and Hines, 2006). As in the experiments of Köndgen *et al.* (Köndgen et al., 2008) and Testa-Silva *et al.* (Testa-Silva et al., 2014), we probed the dynamical transfer properties of each model neuron. We injected a sinusoidally oscillating input current in the soma, allowing us to temporally modulate the instantaneous output firing rate of each model neuron and quantify its output 'transfer gain' (Fig. 4a). When studied in this way, the transfer properties of model neurons resemble those of electronic filters, whose low-pass performances in the Fourier domain define how fast they can follow input changes (for more detailed information see Supplementary Methods).

Action Potential waveform analysis

Action Potential (AP) waveforms were extracted from voltage traces recorded in response to intracellular current injections and sorted according to their instantaneous firing frequency. Instantaneous frequency was determined as 1/time to previous AP. Subsequently all APs were binned in 10Hz bins, while first APs in each trace were isolated in a separate bin. The following AP parameters were calculated for each AP in a train: the AP threshold was calculated as the membrane potential at the point of maximum acceleration of AP (peak of second derivative

(Sekerli et al., 2004). The AP peak voltage was determined as the absolute membrane potential measured at the peak of the AP waveform. The AP amplitude was calculated as the difference in membrane potential between the AP peak voltage and afterhyperpolarization (AHP). AHP was estimated as the lowest membrane potential between AP peak and the initiation of consecutive AP. Maximum rise speed was defined as the peak of AP derivative (dV/dt) and maximum fall speed as the trough of AP derivative. Half-width was estimated as the duration of AP between the voltage points of its half-amplitude (exact voltage at half-amplitude was extrapolated from neighbouring sampling points). For each analysed cell, representative APs with all parameters were plotted for visual check to avoid errors in the analysis.

For each neuron, the mean values of AP parameters in a given frequency bin were obtained by averaging all APs within that frequency bin. Relative AP parameters were calculated by dividing the mean AP parameter in each frequency bin by the mean first AP parameter. For relative threshold estimation, this formula was adjusted to 1 – AP threshold for a given frequency bin/first AP threshold +1 to compensate for negative values. To obtain AP values for each subject, AP parameters within each frequency bin were averaged for all neurons from one subject.

Statistical analysis

Statistical significance of all correlations between parameters was determined using Pearson correlation coefficients using Matlab (version R2017a, Mathworks)

For statistical analysis of AP data, we divided all subjects according to their IQ into 2 groups: group with IQ>100 and a group with IQ<100. Differences between 2 IQ groups in individual AP parameters at different instantaneous frequencies were statistically tested using repeated measures ANOVA (using Matlab).

Since the adaptation of AP parameters at different instantaneous frequencies relative to first AP started already at 10 Hz, we pulled all relative AP parameters for 11-50 Hz bins to have

one measure of each AP parameter per subject. We further performed MANOVA on 7 calculated AP parameters for these 2 groups as dependent variables and IQ scores as independent variables (using IBM SPSS Statistics). We ran subsequent univariate post-hoc tests and used Bonferroni corrected p-value to account for multiple comparisons.

References

Barrett, P., Eysenck, H.J., and Lucking, S. (1986). Reaction time and intelligence: A replicated study. Intelligence *10*, 9–40.

Bekkers, J.M., and Häusser, M. (2007). Targeted dendrotomy reveals active and passive contributions of the dendritic tree to synaptic integration and neuronal output. Proc. Natl. Acad. Sci. U.S.a. *104*, 11447–11452.

Cain, S.M., and Snutch, T.P. (2010). Contributions of T-type calcium channel isoforms to neuronal firing. Channels (Austin) *4*, 475–482.

Carnevale, N.T., and Hines, M.L. (2006). The NEURON Book (Cambridge: Cambridge University Press).

Chklovskii, D.B., Schikorski, T., and Stevens, C.F. (2002). Wiring optimization in cortical circuits. Neuron *34*, 341–347.

Choi, Y.Y., Shamosh, N.A., Cho, S.H., DeYoung, C.G., Lee, M.J., Lee, J.-M., Kim, S.I., Cho, Z.-H., Kim, K., Gray, J.R., et al. (2008). Multiple bases of human intelligence revealed by cortical thickness and neural activation. J. Neurosci. *28*, 10323–10329.

Costales, J., and Kolevzon, A. (2016). The therapeutic potential of insulin-like growth factor-1 in central nervous system disorders. Neurosci Biobehav Rev *63*, 207–222.

Deary, I.J., Penke, L., and Johnson, W. (2010). The neuroscience of human intelligence differences. Nat. Rev. Neurosci. *11*, 201–211.

DeFelipe, J., Alonso-Nanclares, L., and Arellano, J.I. (2002). Microstructure of the neocortex: comparative aspects. J. Neurocytol. *31*, 299–316.

Elston, G.N. (2003). Cortex, cognition and the cell: new insights into the pyramidal neuron and prefrontal function. Cerebral Cortex.

Eyal, G., Mansvelder, H.D., de Kock, C.P.J., and Segev, I. (2014). Dendrites impact the encoding capabilities of the axon. J. Neurosci. *34*, 8063–8071.

Fischl, B. (2004). Automatically Parcellating the Human Cerebral Cortex. Cereb. Cortex *14*, 11–22.

Fischl, B., and Dale, A.M. (2000). Measuring the thickness of the human cerebral cortex from magnetic resonance images. Proc. Natl. Acad. Sci. U.S.a. *97*, 11050–11055.

Hodgkin, A.L., and Huxley, A.F. (1952). Currents carried by sodium and potassium ions through the membrane of the giant axon of Loligo. J. Physiol. (Lond.) *116*, 449–472.

Horikawa, K., and Armstrong, W.E. (1988). A versatile means of intracellular labeling: injection of biocytin and its detection with avidin conjugates. Journal of Neuroscience Methods *25*, 1–11.

Hulshoff Pol, H.E., Schnack, H.G., Posthuma, D., Mandl, R.C.W., Baaré, W.F., van Oel, C., van Haren, N.E., Collins, D.L., Evans, A.C., Amunts, K., et al. (2006). Genetic contributions to

human brain morphology and intelligence. J. Neurosci. *26*, 10235–10242.

Ikari, K., and Hayashi, M. (1981). Aging in the neuropil of cerebral cortex--a quantitative ultrastructural study. Folia Psychiatr Neurol Jpn *35*, 477–486.

Karama, S., Ad-Dab'bagh, Y., Haier, R.J., Deary, I.J., Lyttelton, O.C., Lepage, C., and Evans, A.C. (2009a). Positive association between cognitive ability and cortical thickness in a representative US sample of healthy 6 to 18 year-olds. Neuroimage *47*, S88.

Karama, S., Y, A.-D., Rj, H., Ij, D., Oc, L., C, L., Ac, E., Brain Development Cooperative Group (2009b). Positive association between cognitive ability and cortical thickness in a representative US sample of healthy 6 to 18 year-olds. Intelligence *37*, 145–155.

Köndgen, H., Geisler, C., Fusi, S., Wang, X.-J., Lüscher, H.-R., and Giugliano, M. (2008). The dynamical response properties of neocortical neurons to temporally modulated noisy inputs in vitro. Cereb. Cortex *18*, 2086–2097.

Lam, M., Trampush, J.W., Yu, J., Knowles, E., Davies, G., Liewald, D.C., Starr, J.M., Djurovic, S., Melle, I., Sundet, K., et al. (2017). Large-Scale Cognitive GWAS Meta-Analysis Reveals Tissue-Specific Neural Expression and Potential Nootropic Drug Targets. Cell Rep *21*, 2597–2613.

McDaniel, M. (2005). Big-brained people are smarter: A meta-analysis of the relationship between in vivo brain volume and intelligence. Intelligence *33*, 337–346.

Mohan, H., Verhoog, M.B., Doreswamy, K.K., Eyal, G., Aardse, R., Lodder, B.N., Goriounova, N.A., Asamoah, B., B Brakspear, A.B.C., Groot, C., et al. (2015). Dendritic and Axonal Architecture of Individual Pyramidal Neurons across Layers of Adult Human Neocortex. Cereb. Cortex bhv188.

Narr, K.L., Woods, R.P., Thompson, P.M., Szeszko, P., Robinson, D., Dimtcheva, T., Gurbani, M., Toga, A.W., and Bilder, R.M. (2007). Relationships between IQ and regional cortical gray matter thickness in healthy adults. Cereb. Cortex *17*, 2163–2171.

Nemenman, I., Lewen, G.D., Bialek, W., and de Ruyter van Steveninck, R.R. (2008). Neural coding of natural stimuli: information at sub-millisecond resolution. PLoS Comput. Biol. *4*, e1000025.

Niblock, M.M., Brunso-Bechtold, J.K., and Riddle, D.R. (2000). Insulin-like growth factor I stimulates dendritic growth in primary somatosensory cortex. J. Neurosci. *20*, 4165–4176.

Posthuma, D., De Geus, E.J.C., Baaré, W.F.C., Hulshoff Pol, H.E., Kahn, R.S., and Boomsma, D.I. (2002). The association between brain volume and intelligence is of genetic origin. Nat. Neurosci. *5*, 83–84.

Salinas, E., and Sejnowski, T.J. (2001). Correlated neuronal activity and the flow of neural information. Nat. Rev. Neurosci. *2*, 539–550.

Scholtens, L.H., Schmidt, R., de Reus, M.A., and van den Heuvel, M.P. (2014). Linking macroscale graph analytical organization to microscale neuroarchitectonics in the macaque connectome. J. Neurosci. *34*, 12192–12205.

Sekerli, M., Del Negro, C.A., Lee, R.H., and Butera, R.J. (2004). Estimating action potential thresholds from neuronal time-series: new metrics and evaluation of methodologies. IEEE Trans Biomed Eng *51*, 1665–1672.

Sniekers, S., Stringer, S., Watanabe, K., Jansen, P.R., Coleman, J.R.I., Krapohl, E., Taskesen, E., Hammerschlag, A.R., Okbay, A., Zabaneh, D., et al. (2017). Genome-wide association meta-analysis of 78,308 individuals identifies new loci and genes influencing human intelligence. Nat. Genet. *11*, 201.

Sorrentino, P., Nieboer, D., Twisk, J.W.R., Stam, C.J., Douw, L., and Hillebrand, A. (2017). The Hierarchy of Brain Networks Is Related to Insulin Growth Factor-1 in a Large, Middle-Aged, Healthy Cohort: An Exploratory Magnetoencephalography Study. Brain Connect *7*, 321–330.

Testa-Silva, G., Verhoog, M.B., Goriounova, N.A., Loebel, A., Hjorth, J., Baayen, J.C., de Kock, C.P.J., and Mansvelder, H.D. (2010). Human synapses show a wide temporal window for spike-timing-dependent plasticity. Front Synaptic Neurosci *2*, 12.

Testa-Silva, G., Verhoog, M.B., Linaro, D., de Kock, C.P.J., Baayen, J.C., Meredith, R.M., De Zeeuw, C.I., Giugliano, M., and Mansvelder, H.D. (2014). High bandwidth synaptic communication and frequency tracking in human neocortex. PLoS Biol. *12*, e1002007.

Trampush, J.W., Yang, M.L.Z., Yu, J., Knowles, E., Davies, G., Liewald, D.C., Starr, J.M., Djurovic, S., Melle, I., Sundet, K., et al. (2017). GWAS meta-analysis reveals novel loci and genetic correlates for general cognitive function: a report from the COGENT consortium. Mol. Psychiatry *22*, 336–345.

Tumati, S., Burger, H., Martens, S., van der Schouw, Y.T., and Aleman, A. (2016). Association between Cognition and Serum Insulin-Like Growth Factor-1 in Middle-Aged & Older Men: An 8 Year Follow-Up Study. PLoS ONE *11*, e0154450.

van den Heuvel, M.P., Scholtens, L.H., Feldman Barrett, L., Hilgetag, C.C., and de Reus, M.A. (2015). Bridging Cytoarchitectonics and Connectomics in Human Cerebral Cortex. J. Neurosci. *35*, 13943–13948.

Verhoog, M.B., Goriounova, N.A., Obermayer, J., Stroeder, J., Hjorth, J.J.J., Testa-Silva, G., Baayen, J.C., de Kock, C.P.J., Meredith, R.M., and Mansvelder, H.D. (2013). Mechanisms underlying the rules for associative plasticity at adult human neocortical synapses. J. Neurosci. *33*, 17197–17208.

Verhoog, M.B., Obermayer, J., Kortleven, C.A., Wilbers, R., Wester, J., Baayen, J.C., de Kock, C.P.J., Meredith, R.M., and Mansvelder, H.D. (2016). Layer-specific cholinergic control of human and mouse cortical synaptic plasticity. Nat Commun *7*, 12826.

Vernon, P. (1983). Speed of information processing and general intelligence. Intelligence *7*, 53–70.

Vetter, P., Roth, A., and Häusser, M. (2001). Propagation of action potentials in dendrites depends on dendritic morphology. J. Neurophysiol. *85*, 926–937.

Acknowledgments:

We thank dr. Linda Douw for her assistance with the analysis of brain imaging data and Mr. M. Wijnants for his technical assistance and to the supercomputer facilities CalUA (University of Antwerp) for computing time. N.A.G. received funding for this work from the from the Netherlands Organization for Scientific Research (NWO; VENI grant). H.D.M. received funding for this work from the Netherlands Organization for Scientific Research (NWO; VICI grant), ERC StG “BrainSignals”, and EU H2020 “Human Brain Project” grant agreement no. 604102. M. G. has received funding from EU H2020 “Human Brain Project” no. 720270, and the Flemish Research Foundation (grant no. G0F1517N).

Author contributions:

NAG: performed AP recordings; analysed data; conceived study design; wrote manuscript

D.H contributed to data analysis

R.W. contributed to data analysis

MBV, performed AP recordings and contributed to data analysis

M.G. performed computational modelling

C.V. performed computational modelling

JO and AK: performed AP recordings

HS and MV: contributed IQ data

SI, JCB: performed neurosurgery and provided MRI data

AP; contributed morphology data

CPJdeK: contributed morphology data

MK: contributed IQ data and study design

HDM: conceived study design, wrote manuscript